ENTROPY GENERATION DUE TO NANOFLUID LAMINAR FORCED CONVECTION FLOW THROUGH HEXAGON MICROCHANNEL HEAT SINK

A. A. ALFARYJAT [a], D. STANCIU [a], A. DOBROVICESCU [a], M. ALDHAIDHAWI [a], A.T.GHEORGHIAN [a]

[,a] Faculty of Mechanical Engineering, University Politehnica of Bucharest, 313 Splaiul Independentei, Sector 6, Bucharest, 060042 Romania

*Corresponding author: altayyeb81@yahoo.com

Abstract. Abstract. The effect of using nanofluids SiO_2 with water on generated entropy of a hexagon microchannel heat sink (HMCHS) was numerically investigated in this research. Due to the sensitivity of entropy to duct diameter, hexagon microchannel with hydraulic diameters 278 µm were considered. Incompressible laminar flow regime was assumed. Hexagon MCHS using water as a base fluid with nanofluid (SiO_2) at volume fraction 4% and nanoparticle 25nm. Obtained results signify that SiO_2-H_2O at heat flux 500 kw/m^2 shows lower entropy generation than pure water. Moreover, when Reynolds number increases, frication entropy generation increases and thermal entropy generation and total entropy generation are decreases.

Keywords: Nanofluids, friction entropy generation, thermal entropy generation, total entropy generation, Microchannel heat sink

Nomenclature

c_p	specific heat, (J/(kg.K))
D_h	hydraulic diameter, (µm)
H_{hs}	heat sink height, (µm)
k	thermal conductivity, (W/(m.K))
k_s	solid thermal conductivity,(W/(m.K))
L_{sh}	heat sink length, (µm)
q_w	heat flux, (kW/m^2)
$\dot{S}''_{gen}$	total Generation entropy, (W/K)
$\dot{S}''_{gen,f}$	frictional entropy generation, (W/K)
$\dot{S}''_{gen,th}$	heat transfer entropy generation, (W/K)
T_{in}	inlet temperature (k)
U, V, W	dimensionless velocity in x, y, z coordinates
W_{hs}	*heat sink width,* (µm)
w_{ch}	Microchannel width, (μm)
X, Y, Z	dimensionless cartesian coordinates
U, V, W	dimensionless velocity in x, y, z coordinates
SiO_2	silicon dioxide
Re	Reynolds number

Greek symbols

μ	viscosity, (kg.m/s)
ρ	density, (kg/m^3)
ϕ	particle volume fraction

Subscripts

bf	base fluid
ch	channel
h	hydraulic
hs	heat sink
nf	nanofluid
np	nanoparticle
f	fluid

1. INTRODUCTION

Along with the rapid development of high performance computers, over the last decade, the thermal management of high heat fluxes which are dissipated by microelectronic devices has become a challenging issue. A new method of removing large amounts of heat from small areas is the microchannel heat sink. Tuckerman and Pease [1] have presented the idea of the microchannel heat sink (MCHS), to improve the thermal performance of the electronic devices.

Water flow and heat transfer characteristics are influenced by the microchannel's geometrical parameters, which were numerically investigated by Alfaryjat et al. [2]. This study covers Reynolds number values in the range of 100–1000 when the heat flux is maintained at 500 kW/m^2. It investigates the effects of

three different channel shapes (hexagonal, circular, and rhombus) on the MCHS performance. The investigations found that the hexagonal cross-section MCHS is the best channel shape for the heat transfer coefficient and pressure drop.

The performance of micro-electromechanical systems (MEMS) in heat transfer devices and engines improves as the ability of a fluid medium to transfer large amounts of heat through a minor temperature difference increase, which in turn enhances the efficiency of converting energy in these devices. This circumstance has led to the appearance of a new group of coolants that make use of nanofluids. The heat transfer performance of liquids, including suspended solid nanopowders, was investigated by Choi *et al.* in 1993 [3]. Nanofluids represent a new type of heat conducting fluids which are made up of a base fluid containing suspended nanosized particles, in the range of 1~100 nm. As solid particles exhibit higher thermal conductivity than the conventional base fluid, it is expected that the addition of solid nanoparticles will increase the effective thermal conductivity of the nanofluids.

In addition to the analysis based on basic conservation laws, the second-law analysis is critical to understanding entropy generation attributed to thermodynamic irreversibility, which proves of use in studying the optimum operating conditions when designing a system with less entropy and destruction of available work (exergy) in accordance to the Gouy–Stodola theorem which states that the available work that is lost is directly proportional to entropy generation. Bejan [4] referred to this engineering research method as Entropy Generation Minimization (EGM) and addressed its derivations and applications in a large number of thermal engineering applications.

Tabrizi and Seyf [5] numerically investigated the effect of using Al_2O_3–water nanofluids having different volume fractions and particle diameters on the hydrodynamic performance, generated entropy and heat transfer characteristics of a tangential micro-heat sink (TMHS). It is obvious that, when compared to pure water, nanofluid coolant exhibits a lower total entropy generation rate and, when the volume fraction increases, the total and heat transfer entropy generation rate decreases. Furthermore, it is evident that the frictional contribution of the entropy generation rate increases when the volume fraction increases, which means that when the volume fraction is increased, the system's hydrodynamic efficiency decreases, however the amount of enhancement in frictional entropy is very small, especially at lower Reynolds numbers. A decrease in the diameter of the nanoparticles decreases heat transfer and total entropy generation rates due to the nanofluid's higher thermal conductivity at lower particle diameters, and consequently higher heat transfer enhancement. When increasing the inlet Reynolds number, the frictional irreversibilities of entropy generation rate increase, while the heat transfer contribution and total entropy generation rate decrease. Therefore, a higher inlet Reynolds number results in higher cooling efficiency for the heat sink.

Li and Kleinstreuer [6] studied entropy generation in three trapezoidal microchannels of different sizes for steady laminar flow of pure water and CuO-water nanofluids. It was concluded that the maximum frictional entropy generation rate occurs in particular the middle part of the walls. System entropy generation decreases with the fluid inlet temperature increases. Frictional entropy generation becomes progressively more important when fluid inlet velocity increases.

Hajialigol et al [7] numerically studied mixed convection and performed a second law of thermodynamics analysis for a three-dimensional microchannel filled with a nanofluid exposed to a magnetic field. The results show that the heat transfer increase achieved by increasing the volume fraction is larger at higher Reynolds numbers. The suppression effect of the magnetic field is exhibited only in the central region. The heat transfer from the microchannel walls to the nanofluid also increases as the Hartmann number is increased. Total entropy generation decreases when the magnetic strength and volume fraction increase or the aspect ratio decreases.

Hassan et al [8] theoretically researched how entropy generation is influenced by heat transfer and flow in nanofluid suspensions. The selected fluid model was a conventional nanofluid of alumina-water (Al_2O_3-H_2O). Minichannels- and microchannels with diameters of 3 mm and 0.05 mm were considered, and a laminar flow regime was assumed. It is seen that the entropy generation ratio increases when the solid volume fraction increases. It was observed that the ratio of entropy generation for the nanofluid over the base fluid is higher than unity, and the ratio increases when the solid volume fraction increases. Consequently, the use of the alumina-water nanofluids in microchannels is not recommended. In minichannels, however, the entropy generation rate ratio is less than one and decreases with each increment in the solid volume fraction. Therefore, the application of alumina-water nanofluids to a minichannel is advantageous.

Nasiri et al [9] numerically studied the convection flow of Fe_3O_4-water in a microchannel heat sink with offset fan-shaped reentrant cavities. The results show that the average frictional entropy generation increases and thermal entropy generation decreases as the Reynolds number increases. In addition, the results presented that increasing the magnetic field's power causes a decrease of total entropy generation.

Sohel et al [10] investigated different types of entropy generations in the circular shaped microchannel, and analytically discussed the minichannel using different types of nanoparticles and base fluids. This analysis used Copper (Cu), alumina (Al_2O_3) as the nanoparticle and H_2O, ethylene glycol (EG) as the base fluids. It was found that Cu–H2O nanofluid exhibited the highest decreasing entropy

generation rate ratio (36%) compared to the nanofluids flow through the microchannel at 6 vol.%. The higher thermal conductivity of H_2O results in a much lower thermal entropy generation rate compared to that of the EG base fluid. The fluid friction entropy generation rate decreases by increasing the volume fraction of the nanoparticles. Smaller diameters exhibited less entropy generation in for all nanofluids.

Ting et al [11] investigated the nanofluid entropy generation in asymmetrically heated porous microchannels. The results display that the thermal asymmetries significantly affect the temperature distribution and as a result the heat transfer irreversibility in the system. In addition it was observed that the suspension of nanoparticles decreases the deviation between the thermal equilibrium and non-equilibrium models to less than 10%. In addition, the thermal performance and entropy generation of water–alumina nanofluid flows in porous media embedded in a microchannel under local thermal non-equilibrium condition was also investigated [12]. It was found that, for a high-aspect ratio microchannel, entropy generation decreases with the nanoparticle volume fraction in low-Reynolds-number flow. This trend reverses when the Reynolds number goes above the threshold value, at Re_{th} =100. As a consequence, nanofluid is found to be advantageous over the base fluid only in low-Reynolds-number flow, with a total entropy generation reduction of 16%.

Ting et al [13] analytically studied the effect of streamwise conduction on the entropy generation of low-Peclet-number nanofluid flow in circular microchannel heat sinks under exponentially decaying wall heat flux under constant pumping power conditions. The results show that the nanoparticle suspension increases entropy generation when the heat transfer irreversibility is dominant at a small Peclet number.

Singh et al [14] presented a theoretical investigation of the entropy generation analysis due to flow and heat transfer in nanofluids. Alumina–water nanofluids were the model fluid. They have considered three different tube diameters under different regimes. Those are microchannel (0.1 mm), minichannel (1 mm) and conventional channel (10 mm). It was found that the Al_2O_3-H_2O with high viscosity nanofluids is a better coolant for use in minichannels. Moreover, it was observed that, at lower tube diameters, flow friction irreversibility is more significant and at higher tube diameters, thermal irreversibility is more.

Mah et al [15] analytically reported the effect of viscous dissipation on entropy generation in fully developed laminar forced convection of water–alumina nanofluid in circular microchannels. The results show that, when the viscous dissipation effect is taken into account, the heat transfer coefficient decreases with the nanoparticle volume fraction largely in the nanofluid laminar flow regime in the microchannel. The entropy generation increase induced by increasing the nanoparticle volume fraction is attributed to the increase of both the nanofluid thermal conductivity and viscosity, which causes boosts the heat transfer and fluid friction irreversibilities, respectively.

Based on the above literatures, it is found that there are a very limited number of studies available concerning entropy generation in hexagon microchannel heat sinks operated with nanofluids. In the future, microchannel heat sinks which use nanofluids are expected to be good candidates for cooling devices. This paper focuses on entropy generations in a hexagon microchannel system with nanofluids in laminar flow, where the irreversibility's friction and heat transfer factors were considered.

2. METHODOLOGY

The calculation aspect of this study evaluates the entropy generation analysis for hexagon microchannels. This section presents the input data and mathematical equations. For the input data, the section includes the hexagon MCHS diagram and the material properties. The mathematical equations section includes the equation to measure the nanofluid's thermo-physical properties and entropy generation. The entropy generation equation for the Hexagon microchannel heat sink was taken from Li and Kleinstreuer [6]. Fig. 1 shows the microchannel heat sink diagram and illustrates the nanofluid flow through a hexagon microchannel having a constant cross section and a hydraulic diameter of 278 μm. For the symmetry advantage, a control volume (channel 14) is selected to study the entropy generation model. The dimensions of the microchannel heat sink and the hexagon cross-section shape are given in Table 1. The top surface of all control volumes is heated with a different heat flux of (125, 200 and 500) kw/m^2. The bottom of the control volume is thermally insulated and the side walls are symmetrical. The water inlet temperature is 290 K. The Reynolds number for all channel cross sections varies between 100 and 1500.

	Hexagon
L (μm)	10,000
W (μm)	22,000
H (μm)	1500
Dh (μm)	278
W_{ch} (μm)	788

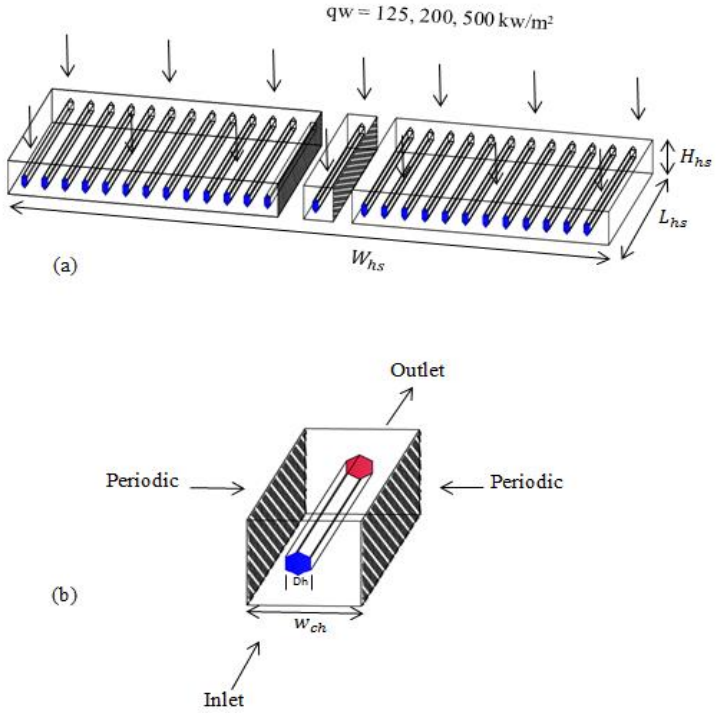

Fig. 1. (a) Schematic diagram of the computational domain, (b) Microchannel heat sink

2.3 Governing equations

The computing domain consists of a fluid and a solid part. In the fluid part the flow is laminar and governed by the Navier-Stokes equation system involving all continuity, momentum and energy equations. Since the fluid is incompressible and the thermo-physical properties are considered constant with respect to the temperature, the energy equation is uncoupled from the continuity and momentum equations. In the solid part of computing domain only the energy equation is needed to model the temperature field

The non-dimensional governing equations of continuity, momentum and energy are [16]:

The Continuity equation is:

$$\frac{\partial U}{\partial X}+\frac{\partial V}{\partial Y}+\frac{\partial W}{\partial Z}=0 \tag{1}$$

The X-Momentum equation is:

$$U\frac{\partial U}{\partial X}+V\frac{\partial U}{\partial Y}+W\frac{\partial U}{\partial Z}=$$
$$=-\frac{dp}{dX}+\frac{1}{\mathrm{Re}}+\left(\frac{\partial^2 U}{\partial X^2}+\frac{\partial^2 U}{\partial Y^2}+\frac{\partial^2 U}{\partial Z^2}\right) \tag{2}$$

The Y-Momentum equation is:

$$U\frac{\partial V}{\partial X}+V\frac{\partial V}{\partial Y}+W\frac{\partial V}{\partial Z}=$$
$$=-\frac{dp}{dY}+\frac{1}{\mathrm{Re}}+\left(\frac{\partial^2 V}{\partial X^2}+\frac{\partial^2 V}{\partial Y^2}+\frac{\partial^2 V}{\partial Z^2}\right) \tag{3}$$

The Z-Momentum equation is:

$$U\frac{\partial W}{\partial X}+V\frac{\partial W}{\partial Y}+W\frac{\partial W}{\partial Z}=$$
$$=-\frac{dp}{dY}+\frac{1}{\mathrm{Re}}+\left(\frac{\partial^2 W}{\partial X^2}+\frac{\partial^2 W}{\partial Y^2}+\frac{\partial^2 W}{\partial Z^2}\right) \tag{4}$$

The energy equation is:

$$U\frac{\partial \theta}{\partial X}+V\frac{\partial \theta}{\partial Y}+W\frac{\partial \theta}{\partial Z}=$$
$$=-\frac{1}{\mathrm{Re}.\mathrm{Pr}}\left(\frac{\partial^2 \theta}{\partial X^2}+\frac{\partial^2 \theta}{\partial Y^2}+\frac{\partial^2 \theta}{\partial Z^2}\right) \tag{5}$$

The dimensionless parameters are:

$$X=\frac{x}{D_h},Y=\frac{y}{D_h},Z=\frac{z}{D_h},$$
$$U=\frac{u}{u_{in}},V=\frac{v}{u_{in}},W=\frac{w}{u_{in}}.$$

2.1. Thermophysical Properties of Nanofluid

The thermophysical properties of the water and the SiO_2-H_2O nanofluids (volume fraction 4% and

nanoparticle 25 nm) at 290 K are listed in Table 2. The nanofluid's physical properties equations, such as density, thermal conductivity, heat capacity and viscosity can be obtained from the following equation, as stated by Ghasemi and Aminossadati [16]:

$$\rho_{nf} = (1-\phi)\rho_{bf} + \phi\rho_{np} \quad (6)$$

$$(\rho c_p)_{nf} = (1-\phi)(\rho c_p)_{bf} + \phi(\rho c_p)_{np} \quad (7)$$

$$(\rho\beta)_{nf} = (1-\phi)(\rho\beta)_{bf} + \phi(\rho\beta)_{np} \quad (8)$$

Nanofluids thermal conductivity has been obtained by Vajjha et al. [17]:

$$k_{eff} = k_{static} + k_{brownian} \quad (9)$$

$$k_{static} = k_{bf}\left[\frac{k_{np} + 2k_{bf} - 2(k_{bf} - k_{np})\phi}{k_{np} + 2k_{bf} + (k_{bf} - k_{np})\phi}\right] \quad (10)$$

$$k_{brownian} = 5\times10^4 \beta\phi\rho_{bf}c_{p.bf}\sqrt{\frac{kT}{2\rho_{np}R_{np}}}.f(T,\phi) \quad (11)$$

$$k = 1.3807\times10^{-23}\ \frac{J}{k} \quad (12)$$

Modeling function (SiO2), β:

$$\beta = 1.9526(1000\phi)^{-1.4594} \quad (13)$$

Modeling function *(T, Ø)* [40].

$$f(T,\phi) = (2.8217\times10^{-2}\phi + 3.917\times10^{-3})\left(\frac{T}{T_o}\right) + \\ + (-3.0699\times10^{-2}\phi - 3.91123\times10^{-3}) \quad (14)$$

The effective viscosity equation of the nanofluids can be calculated based on Corcione [18].

$$\frac{\mu_{eff}}{\mu_{bf}} = \frac{1}{1-34.87\left(\frac{d_{np}}{d_{bf}}\right)^{-0.3}\phi^{1.03}} \quad (15)$$

$$d_{bf} = \left[6M/(N\pi\rho_{bf})\right]^{1/3} \quad (16)$$

***Table 2**: Thermophysical properties of water and nanoparticle SiO_2.*

Properties	*H_2O*	*SiO_2*	*SiO2-H2O*
Density, ρ (kg/m³)	998.2	2200	1010.812
Specific heat, cp (J/kgK)	4187	703	4111.1719
Thermal conductivity, k (W/mK)	0.6	1.2	0.6056101
Dynamic viscosity, μ (Ns/m²)	0.001003	-	0.0011827

2.3. Entropy Generation of Nanofluid

In the convection process, the overall rate of volumetric entropy generation equation is linked as.

$$\dot{S}_{gen} = \iiint_{\Omega} \dot{S}'''_{gen} d\Omega \quad (17)$$

Where Ω represent the computing volume, obviously it consists of fluid and solid parts. For the solid parts only the thermal term of entropy generation equation is computed [17]:

$$\dot{S}'''_{gen} = \dot{S}'''_{gen,th} + \dot{S}'''_{gen,f} \quad (18)$$

$$\dot{S}'''_{gen,th} = \frac{k}{T^2}\left[\left(\frac{\partial T}{\partial x}\right)^2 + \left(\frac{\partial T}{\partial y}\right)^2 + \left(\frac{\partial T}{\partial z}\right)^2\right] \quad (19)$$

$$\dot{S}'''_{gen,f} = \frac{\mu}{T}\phi, \quad (20)$$

where ϕ is the frictional dissipation function and it's computed as follow [17]:

$$\phi = \left(\begin{array}{l} 2\left[\left(\frac{\partial u}{\partial x}\right)^2 + \left(\frac{\partial v}{\partial y}\right)^2 + \left(\frac{\partial w}{\partial z}\right)^2\right] + \\ + \left(\frac{\partial u}{\partial y} + \frac{\partial v}{\partial x}\right)^2 + \left(\frac{\partial u}{\partial z} + \frac{\partial w}{\partial x}\right)^2 + \left(\frac{\partial v}{\partial z} + \frac{\partial w}{\partial y}\right)^2 \end{array}\right) \quad (21)$$

2.5 Numerical procedure

The calculations pertaining to the numerical simulations were carried out by solving the governing conservation equations (Equations. (1) – (5)) using the finite volume method (FVM) together with the corresponding boundary conditions [18].The equations used for both the solid and fluid phase were solved simultaneously

as a single domain conjugate problem. The MCHS' flow field was solved using the SIMPLEC algorithm [19]. The geometry of the CFD region was determined and the mesh was generated using the GAMBIT program. By applying the CFD techniques, geometrical parameters' effects on the MCHS were investigated, water being used as the base fluid. For the convective terms, the second-order upwind differencing scheme was considered. Finding the velocity components required solving the momentum equation. The continuity equation was used to update the pressure. The continuity equation does not have any pressure, but it can be easily transformed into a pressure correction equation. The convergence criterion required that the relative maximum mass residual dependent on the inlet mass be smaller than 1 and the velocity components did not change from iteration to iteration.

3. RESULTS

3.1. Friction Entropy Generation:

Fig. 1 shows the overall rate variation of the friction entropy generation rate inside the micro-channel for both fluids. Since the fluid thermos-physical properties are considered constant, the value of q_w does not influence the velocity fields. As a result the variations are the same for all values of heat flux. As expected, the overall rate of friction entropy generation increases with respect to Re number. In the same time, the values of $S_{gen,f}$ are greater for nano-fluid than for pure water and the difference between them grows with Re. From fig. 1 one may find that, at Re=1400, the nano-fluid flow creates a friction irreversibility five time greater than the pure water flow. This behaviour is due to the higher value of nano-fluid viscosity which at its turn determines higher velocity gradients than in the case of pure water flow. Cleary the nano-fluid flows determine lower frictional efficiencies than the flows of pure water.

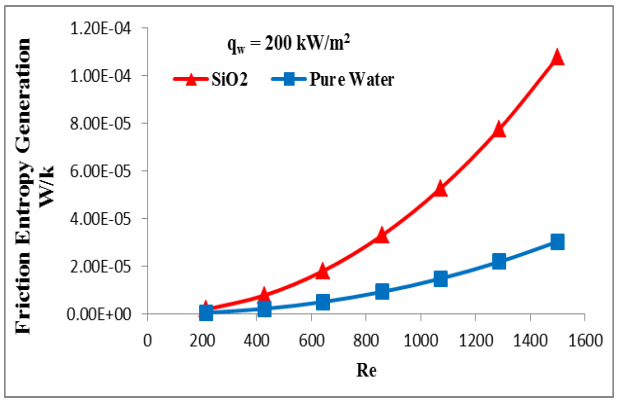

Fig.2. Frictional entropy generation rate as a function of Reynolds number for different heat flux.

3.2. Thermal Entropy Generation:

Fig. 2 a-c shows the thermal entropy generation rate in a hexagon microchannel heat sink for nanofluid SiO_2-H_2O and pure water for different heat fluxes. The results indicated that the thermal entropy generation decreases when the heat flux decreases. Moreover, SiO_2-H_2O shows lower thermal entropy generation than pure water. This is due to the high thermal conductivity of this nanofluid, which, for a given q_w, determines lower temperature gradients. As the Reynolds number is growing, as the temperature gradients, as well as the temperature levels are diminishing, so that the increase of Reynolds number lead to decrease the overall rate of thermal entropy generation component.

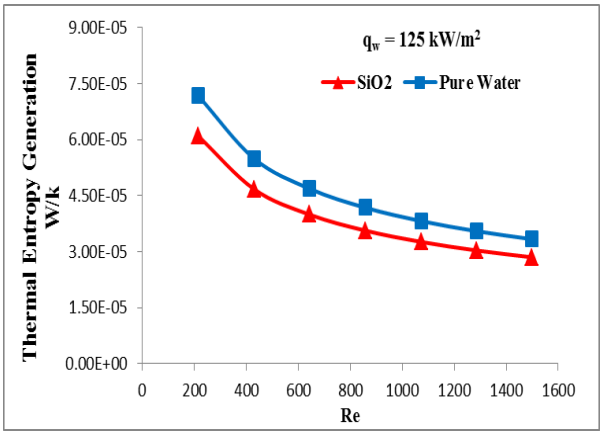

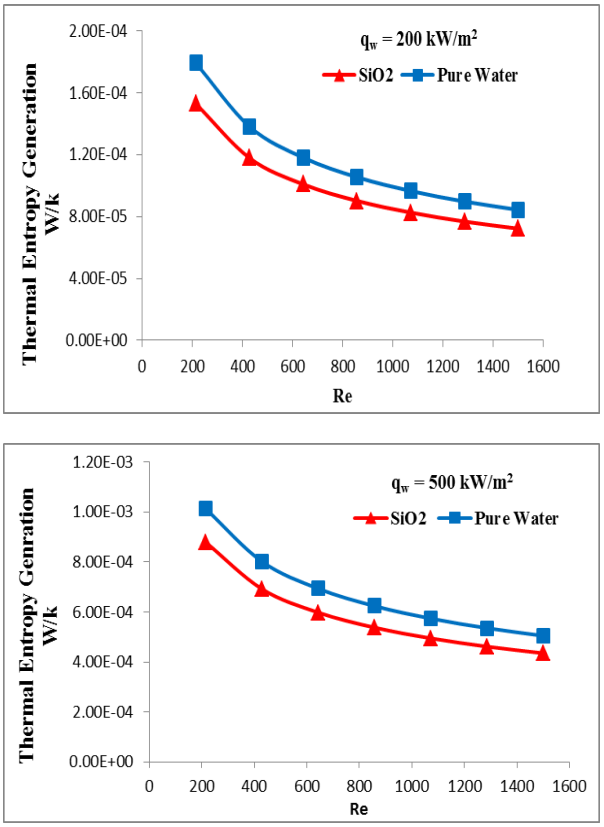

Fig. 3. Thermal entropy generation as a function of Reynolds number for different heat flux

3.3. Total Entropy Generation

The overall rate of the total entropy generation of SiO_2-H_2O and pure water for different heat flux is showed in Fig. 3 a,b,c. For heat fluxes between 125 and 500 kW/m^2, the results appeared that the SiO_2-H_2O has lower entropy generation than pure water in Reynolds number range from 100 to 1400, then pure water value shows lower entropy generation than SiO_2-H_2O. The Re number, Re_{eq}, for which the two fluids generate the same irreversibility is growing as q_w increases. At lower values of q_w, the overall irreversibility is dominated by the thermal component in a narrow Reynolds number interval. Beyond it, the viscous component prevails. The Re interval of thermal dominated irreversibility enlarge as the q_w grows because the overall rate of thermal entropy creation increases while, the overall rate of viscous entropy generation remains unchanged. On the other hand, one have previously seen that $S_{gen,th}$ is always lower for nanofluid than for water while the $S_{gen,f}$ is always higher. So, the trade of between these irreversibility components determines the growth of Re_{eq} for which the overall rate of entropy generation is the same for both fluids. At lower values than Re_{eq}, the nanofluid have to be chosen while at higher values the pure water have to be used in order to lower the overall irreversibility. When targeting the minimum value of entropy generation one has to select one of the two considered fluids depending on q_w level.

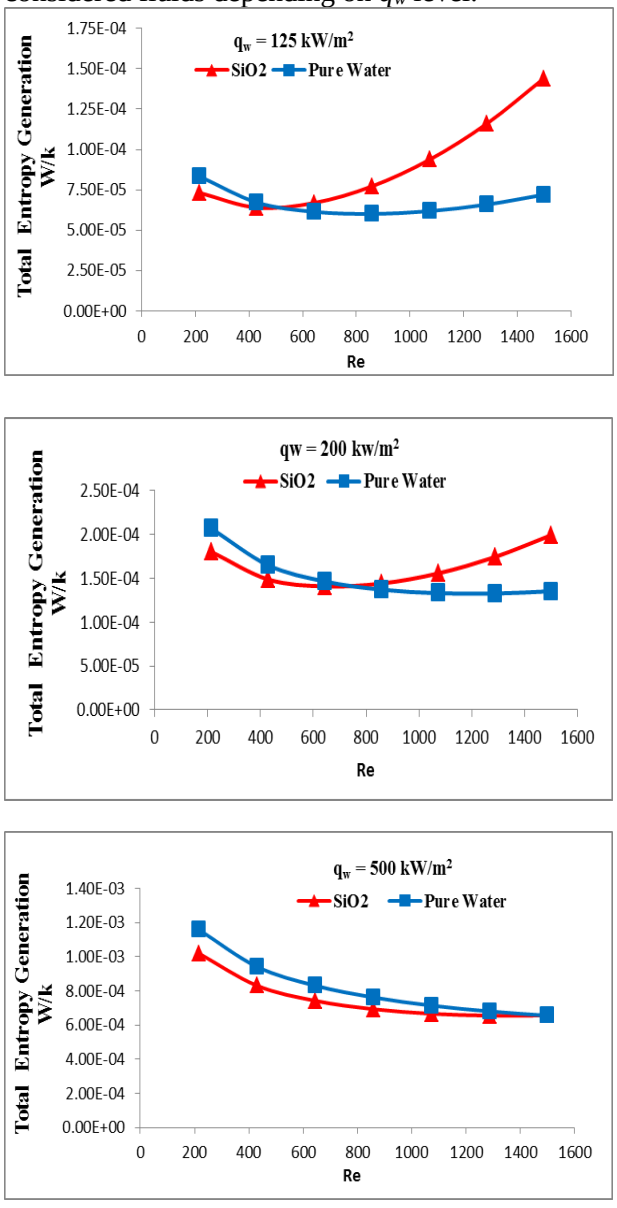

Fig. 4. Total Entropy generation rate as a function of Reynolds number for different heat flux

4. CONCLUSION

The effects of nanofluid (SiO_2-H_2O) on entropy generation of hexagon microchannel heat sink are analyzed in this work. 3D governing equations of laminar and incompressible fluid flow have been solved using finite volume method. Based on the

above simulated results, the following conclusions can be drawn:

- Friction entropy generation of nanofluids show higher value than pure water for different heat flux, also when heat flux increase the friction entropy generation keep constant.
- Increasing heat flux caused increasing in the thermal entropy generation and total entropy generation.
- SiO_2-H_2O nanofluid show lower thermal entropy generation than pure water for different heat flux.
- For the heat flux 125 and 200 kw/m^2, SiO_2-H_2O appeared lower results than pure water for Reynolds number between 100 to 700, and it increases when Reynolds number increases.
- At heat flux 500 kW/m^2, the total entropy generation of nanofluid SiO_2-H_2O shows lower value than pure water for Reynolds number varying between 100 to 1500.

ACKNOWLEDGEMENT

The present work has been supported by the Romanian government through Research grant," Hybrid micro-cogeneration group of high efficiency equipped with an electronically assisted ORC", 2nd National Plan, Grant Code: PN-II-PT-PCCA-2011-3.2-0059, Grant No.: 75/2012.

REFERENCES

[1] Tuckerman D.B., Pease R.F., High performance heat sinking for VLSI, IEEE Electron. Devices Lett. EDL-2, 126-129, 1981].

[2] Alfaryjat A.A., Mohammed H.A., Adam N.M., Ariffin M.K.A., Najafadi M.I., Influence of geometrical parameters of hexagonal, circular, and rhombus microchannel heat sinks on the thermohydraulic characteristics, *International Communications in Heat and Mass Transfer.*, **52**, 121–131, 2014.

[3] Choi, S.U.S.; Eastman, J. *Enhancing Thermal Conductivity of Fluids with Nanoparticles*; Argonne National Lab.: Argonne, Illinois, USA, 1995.

[4] A. Bejan, Entropy Generation Minimization, CRC Press, Boca Raton, 1995.

[5] Tabrizi A.S., Seyf H.R., Analysis of entropy generation and convective heat transfer of Al2O3 nanofluid flow in a tangential micro heat sink, *International Journal of Heat and Mass Transfer*, **55**, 4366–4375, 2012.

[6] Li J., Kleinstreuer .C., Entropy Generation Analysis for Nanofluid Flow in Microchannels, *Journal of Heat Transfer.*, **132**, 122401-1, 2010.

[7] Hajialigol N., Fattahi A., Ahmadi M.H., Qomi M.E., Kakoli E., MHD mixed convection and entropy generation in a 3-D microchannel using Al_2O_3–water nanofluid, *Journal of the Taiwan Institute of Chemical Engineers.*, **46**, 30–42, 2015.

[8] Hassan M., Sadri R., Ahmadi G., Dahari M.B., Kazi S.N., Safaei M.R., Sadeghinezhad E., Numerical Study of Entropy Generation in a Flowing Nanofluid Used in Micro- and Minichannels, *Entropy*, **15**, 144-155, 2013.

[9] Nasiri M., Rashidi M.M., Lorenzini G., Effect of Magnetic Field on Entropy Generation in a Microchannel Heat Sink with Offset Fan Shaped, *Entropy*, **18,** 10, 2016.

[10] Sohel M.R., Saidur R., Hassan N.H., Elias M.M., Khaleduzzaman S.S., Mahbubul I.M., Analysis of entropy generation using nanofluid flow through the circular microchannel and minichannel heat sink, *International Communications in Heat and Mass Transfer*, **46**, 85–91, 2013.

[11] Ting T.W., Hung Y.M., Guo N., Entropy generation of viscous dissipative nanofluid convection in asymmetrically heated porous microchannels with solid-phase heat generation, *Energy Conversion and Management*, **105**, 731–745, 2015.

[12] Ting T.W., Hung Y.M., Guo N., Entropy generation of viscous dissipative nanofluid flow in thermal non-equilibrium porous media embedded in microchannels, *International Journal of Heat and Mass Transfer*, **81**, 862–877, 2015.

[13] Ting T.W., Hung Y.M., Guo N., Entropy generation of nanofluid flow with streamwise conduction in microchannels, *Energy*, **64** 979-990, 2014.

[14] Singh P.K., Anoop K.B., Sundararajan T., Das S.K., Entropy generation due to flow and heat transfer in nanofluids, *International Journal of Heat and Mass Transfer*, **53**, 4757–4767, 2010.

[15] Mah W.H., Hung Y.M., Guo N., Entropy generation of viscous dissipative nanofluid flow in microchannels, *International Journal of Heat and Mass Transfer*, **55**, 4169–4182, 2012.

[16] Ghasemi B., Aminossadati S.M., Brownian motion of nanoparticles in a triangular enclosure with natural convection, *International Journal of Thermal Sciences*, **49**, 931-940, 2010.

[17] Vajjha, R. S., Das, D. K., and Kulkarni, D. P, Development of new correlations for convective heat transfer and friction factor in turbulent regime for nanofluids. *International Journal of Heat and Mass Transfer*, **53**, 4607-4618, 2010.

[18] Corcione M., Heat transfer features of buoyancy-driven nanofluids inside rectangular enclosures differentially heated at the sidewalls, *International Journal of Thermal Sciences*, **49**, 1536-1546, 2010.